Spin-valve magnetization reversal obtained by N-doping in Fe/insulator/Fe trilayers

2003 J. Phys.: Condens. Matter 15 617

(http://iopscience.iop.org/0953-8984/15/4/302)

INSTITUTE OF PHYSICS PUBLISHING JOURNAL OF PHYSICS: CONDENSED MATTER

J. Phys.: Condens. Matter **15** (2003) 617–624 PII: S0953-8984(03)52297-4

Spin-valve magnetization reversal obtained by N-doping in Fe/insulator/Fe trilayers

M T Georgieva[1], N D Telling[1,3], G A Jones[1], P J Grundy[1], T P A Hase[2] and B K Tanner[2]

[1] Joule Physics Laboratory, Institute for Materials Research, University of Salford, Salford M5 4WT, UK
[2] Department of Physics, University of Durham, South Road, Durham DH1 3LE, UK

E-mail: n.telling@physics.org

Received 13 August 2002
Published 20 January 2003
Online at stacks.iop.org/JPhysCM/15/617

Abstract

The effect of N-doping on the microstructure and coercivity of the 'free' Fe layer in Fe/insulator/Fe trilayers has been examined. It was found that N-doping leads to a magnetic softening of the Fe layer and a corresponding reduction in the grain size. Hard/soft spin-valve trilayers, showing good independent layer reversal, were obtained using N-doped and undoped Fe layers. Ferromagnetic interlayer coupling was found in these trilayers that could be well described by a Néel coupling mechanism. Nonuniform reversal of the harder Fe layer, once incorporated in the trilayer, was also observed and could be reproduced using a simple model in which local variations in the interlayer coupling energy are considered. Such variations are likely to be caused by structural inhomogeneity in the films. N-doping is potentially important as a method for tailoring the coercivity of the 'free' layer in spin-valves comprising high-polarization magnetic materials.

1. Introduction

The development of the giant-magnetoresistance (GMR) and tunnelling magnetoresistance (TMR) effects in spin-valve magnetic multilayers has led to considerable interest in the magnetization reversal processes in these film systems [1–5]. It is these processes that determine the field sensitivity of the magnetoresistance (MR) and are thus extremely important for potential device applications. In order to obtain substantial MR ratios, high-polarization metals (such as Fe and Co) are required for the ferromagnetic layers adjacent to the spacer [6, 7]. However, the coercivity of these materials is larger than ideal if they are to be used as the 'free' magnetic layer in spin-valves. Thus, instead, alloys such as NiFe are typically employed [3, 4, 8]. In this paper the use of N-doping to reduce the coercivity in the 'free' Fe

[3] Author to whom any correspondence should be addressed.

layer in Fe/insulator/Fe trilayers is discussed. It is shown that the use of N-doping enables the preparation of pseudo-hard/soft spin-valves with good independent reversal of the Fe layers.

It is well known that interlayer coupling affects the layer reversal in spin-valve systems [1, 3, 4, 9]. Magnetometry measurements discussed here suggest the presence of a degree of such coupling in these N-doped trilayers. By employing a suitable magnetostatic coupling model [10], and using structural parameters obtained by a thorough structural refinement of the films, it is shown that the coupling is well described by a Néel coupling mechanism [11]. It is also shown that the appearance of nonuniform reversal of the Fe layers, once incorporated in the trilayers, can be ascribed to local variations in the coupling energy across the film area.

2. Experiment

All films were grown on Si(100) wafers in a high-vacuum thin-film deposition system, at a base pressure $\leqslant 10^{-8}$ mbar. Fe layers were prepared by magnetron sputtering in an Ar partial pressure of 2×10^{-3} mbar. Insulating spacer layers of AlN were prepared by first sputtering a thin Al layer, and then reacting it with N by exposure to a N atomic (free radical) beam from an *Oxford Applied Research* RF atom source. N-doped Fe layers were obtained by magnetron sputtering as before, but with the addition of a 5×10^{-5} mbar partial pressure of N_2 to the sputtering gas.

Initially single layers of N-doped and undoped Fe of different thicknesses were prepared on Si(100) substrates. A set of trilayer films were subsequently prepared with the design structure: Si(100)/Fe(200 Å)/AlN(40 Å)/Fe*(x Å), where the Fe* designates the N-doped Fe layer, and x was varied in the range 200–600 Å. Magnetometry was performed on all samples at room temperature using a vibrating sample magnetometer (VSM). Structural characterization was achieved through a combination of transmission electron microscopy measurements (TEM) and x-ray reflectivity. The latter measurements were obtained using a dedicated *Bede* reflectometer at the University of Durham, operating at a wavelength of 1.393 Å. Cross-sectional and planar TEM specimens were prepared using a combination of mechanical polishing and Ar ion milling. Observations were made using JEOL 200CX and high-resolution JEOL 3010 microscopes.

3. Results and discussion

M–H loops obtained from the single Fe layers of different thicknesses are shown in figure 1. The undoped Fe film (figure 1(a)) shows a sharp, isotropic reversal that is typical of the sputtered Fe films. In comparison to this, the N-doped films (figures 1(b)–(d)) show a dramatic reduction in coercivity, and the appearance of a weak in-plane uniaxial anisotropy. In order to investigate the origin of these changes, the microstructure and electron diffraction patterns from planar specimens were observed by TEM, as shown in figure 2. The formation of FeN phases in the films might be thought to be responsible for the change in coercivity, as these have been shown previously to be magnetically soft [12, 13]. However, it can be seen from the diffraction patterns that no significant FeN phases have formed in the film as only a bcc α-Fe pattern is observed. Instead, it seems the reduction in coercivity is associated with the finer grain structure ($\lesssim$100 Å average in-plane grain size in the N-doped films compared to $\sim$200 Å otherwise) caused by the increased nucleation rate in the presence of nitrogen.

In nanocrystalline magnetic films (with grain sizes $\lesssim$100 Å) a low coercivity is often observed as the result of an averaging of the magnetocrystalline anisotropy by the ferromagnetic exchange interaction [14]. For this to occur, the grain boundaries must be sufficiently thin and

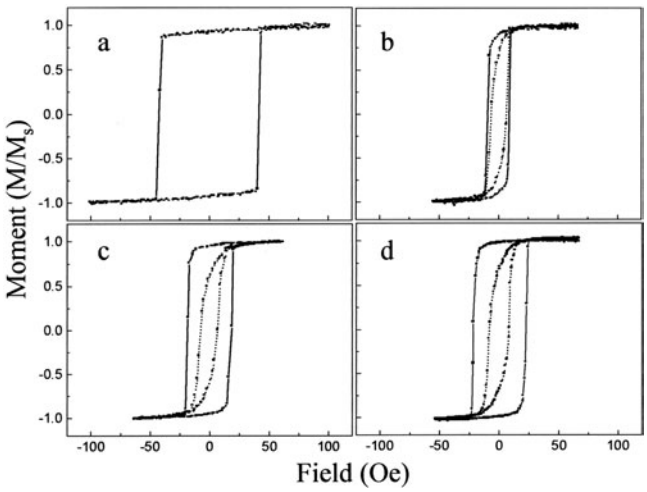

Figure 1. Easy-axis (solid curves) and hard-axis (broken curves) M–H loops obtained by VSM from: (a) 200 Å undoped Fe film, (b) 200 Å N-doped Fe film, (c) 400 Å N-doped Fe film and (d) 600 Å N-doped Fe film. The film in (a) was found to be isotropic in-plane and so only one loop is shown.

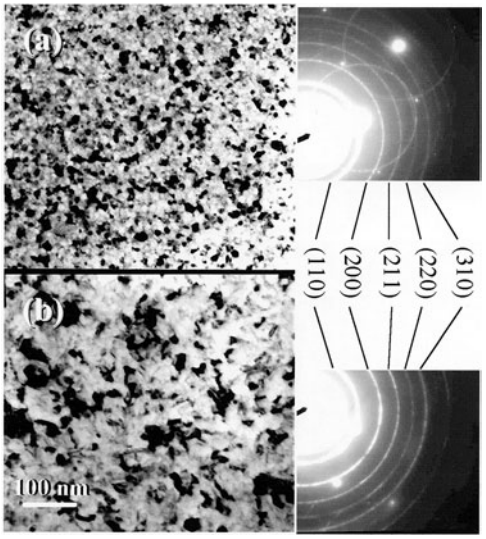

Figure 2. TEM bright-field micrographs (left) and electron diffraction patterns from (a) N-doped 200 Å Fe film, (b) undoped 200 Å Fe film.

ferromagnetic to enable strong intergranular coupling via the exchange interaction. This is likely to be the case for the single-phase α-Fe films shown here. The weak induced uniaxial anisotropy that is also observed may be caused by the anisotropic ordering of interstitial N dissolved in the films. This effect has been studied in bulk iron samples [15] and has been seen previously in FeAl(N) alloy films [16].

The major and minor M–H loops obtained from the set of Fe/AlN/Fe* trilayer films are shown in figure 3. It can be seen that a hard/soft-spin-valve reversal, with good independent reversal of the magnetic layers, has been obtained by N-doping the upper Fe layer. This magnetic 'softening' of the upper (Fe*) layer was achieved through grain refinement of the microstructure, which is preferable to alloy formation as it preserves the Fe polarization. The

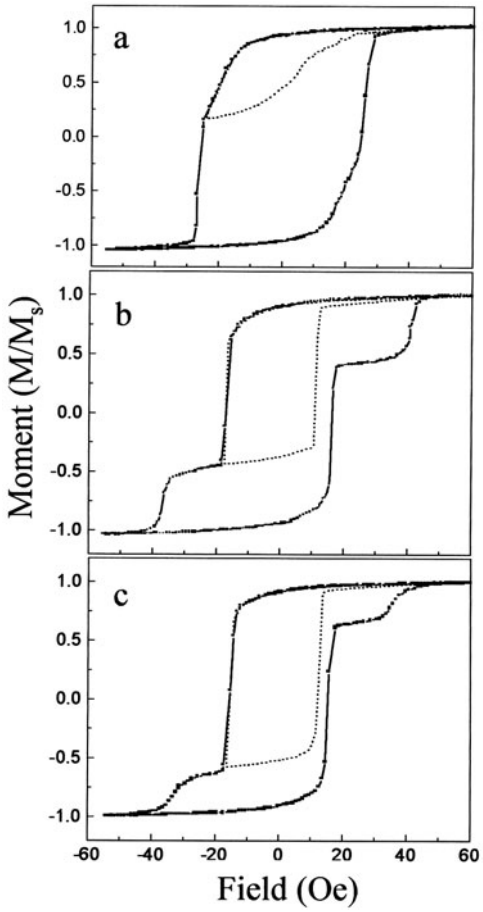

Figure 3. Major (solid curves) and minor (broken curves) M–H loops obtained by VSM from the set of trilayer films with the nominal structure Si(100)/Fe(200 Å)/AlN(40 Å)/Fe*(x Å), where Fe* indicates a N-doped layer and x is (a) 200 Å, (b) 400 Å and (c) 600 Å.

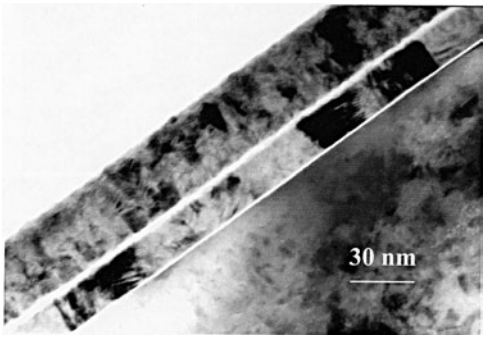

Figure 4. A cross-sectional TEM image taken from a trilayer film with the nominal structure Si(100)/Fe(200 Å)/AlN(40 Å)/Fe*(400 Å). The AlN spacer (bright contrast) can be seen clearly separating the lower Fe (larger-grained) and upper Fe* (smaller-grained) layers.

difference in microstructure and grain sizes of the upper (Fe*) and lower (Fe) layers is evident in the TEM cross-sectional image, shown in figure 4, in which the formation of a high-quality AlN spacer layer can also be seen.

The shift in the origin of the minor loops with respect to the centre of the major loops, shown in figure 3, is indicative of ferromagnetic interlayer coupling between the Fe layers. This coupling is likely to have a magnetostatic origin, as indirect exchange coupling is expected to be minimal due to the band structure of the insulating spacer. Several mechanisms that lead to

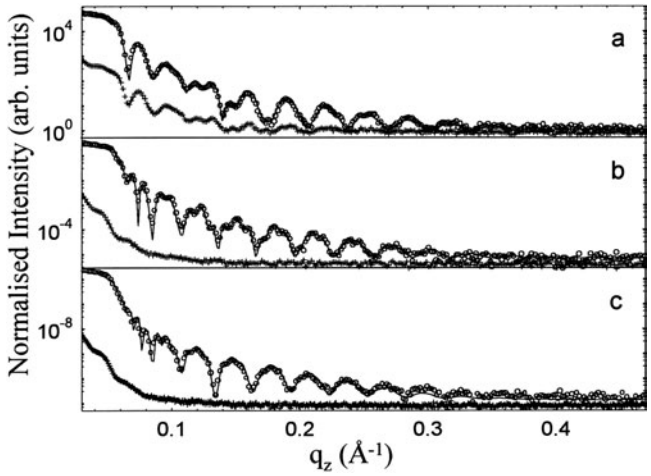

Figure 5. The specular x-ray reflectivity (open circles) and best-fit simulation (solid curve) for the set of trilayer films with nominal structure Si(100)/Fe(200 Å)/AlN(40 Å)/Fe*(*x* Å), where Fe* indicates a N-doped layer and *x* is (a) 200 Å, (b) 400 Å and (c) 600 Å. The off-specular data (crosses) are the curves below the specular data in each case.

such a ferromagnetic coupling have been proposed, including domain wall coupling [17] and Néel or 'orange peel' coupling [11]. With the exception of that for the sample with the thinnest Fe* layer (figure 3(a)), the minor loops are symmetric about their centre (figures 3(b) and (c)) and have coercivities less than those of the equivalent single films (shown in figure 1). It is unlikely, therefore, that domain wall coupling plays a dominant role in the interlayer coupling in these films as this would be expected to increase the coercivity of the minor loop [4]. However, as the interlayer coupling *energy* is a surface energy density [9, 11], the coupling *field* experienced by the Fe* layer increases as its thickness decreases. Thus for the trilayer with the thinnest Fe* layer, this leads to similar switching fields for the Fe and Fe* layers (figure 3(a)). In this case, domains may nucleate in the hard layer during the soft-layer reversal and it is thus more likely that domain wall coupling could play a role. This is reflected in the asymmetric nature of the minor loop in figure 3(a).

Néel coupling is caused by the interfacial roughness at the boundaries of the magnetic layers and requires that the interfaces be correlated. In order to determine the average interfacial structure of the films over the whole sample area, x-ray reflectivity measurements were performed. The results of the specular and off-specular (longitudinal) measurements are given in figure 5. The specular data were fitted using the *Bede Mercury* code [18] based on a dynamical formulism incorporating the distorted wave Born approximation. Good fits to the data were obtained by analysing the sample set self-consistently, and the fitted parameters obtained are given in table 1. Although specular reflectivity cannot distinguish between true interface roughness and interdiffusion, similar surface roughness amplitudes have been measured by atomic force microscopy (not shown). Thus the sizable interfacial amplitudes measured are predominantly due to rough boundary interfaces rather than interdiffused layers.

The replication of the reflectivity fringes in the off-specular data for the sample with the thinnest Fe* layer (figure 5(a)) clearly indicates that a significant portion of the interface roughness is correlated over the entire sample thickness, including through the spacer layer which is a requirement for Néel coupling to occur. The roughness amplitudes obtained from the fits to the specular data (table 1) imply that the roughness is cumulative (increases towards

Table 1. Layer thickness and interface roughness amplitudes obtained from fits to the specular x-ray reflectivity data (the symbols are defined in the text). The interface roughness amplitude, h_3, defines the upper film surface, and an additional Fe_2O_3 surface oxide layer was required in the simulations to improve the fit. Also shown are the average grain size (λ), the measured shift of the minor loop in the VSM curves and the estimated Néel coupling field on the Fe* layer, H_f.

			Interface roughness amplitude (Å)					Shift of minor	
t_f (Å)	t_h (Å)	t_s (Å)	h_0	h_1	h_2	h_3	λ (Å)	loop (Oe)	H_f (Oe)
163 ± 2	190 ± 1	43 ± 1	4.9 ± 0.5	6.9 ± 0.7	16.7 ± 1.4	22 ± 1	200	7.0 ± 0.5	6.2
365 ± 4	200 ± 1	41 ± 2	4.9 ± 0.5	6.4 ± 0.9	17 ± 2	23 ± 2	200	3 ± 0.5	3.1
565 ± 5	204 ± 1	42 ± 2	4.9 ± 0.7	7 ± 1	19 ± 2	25 ± 2	200	1.5 ± 0.5	1.9

the surface). The deposition of thicker Fe* layers results in a rougher surface which is no longer correlated with the lower layers. Thus, as the upper Fe layer thickness increases (figures 5(b) and (c)), the correlations of the lower interfaces are maintained, but the out-of-plane correlation length is now less than the total film thickness and the off-specular fringes are lost.

An estimation of the coupling field on the free layer, H_f, can be obtained in the case of a spin-valve with an upper free layer of thickness, t_f, and possessing cumulative roughness [10, 11], according to the expression

$$H_f = \frac{\pi^2 h_1 h_2 M_h}{\sqrt{2}\lambda t_f} \exp\left(\frac{-2\sqrt{2}\pi t_s}{\lambda}\right)\left[1 - \left(\frac{h_0}{h_2}\right)\exp\left(\frac{-2\sqrt{2}\pi t_h}{\lambda}\right)\right] \qquad (1)$$

where h_0 is the amplitude of roughness at the substrate/hard-layer interface, h_1 and h_2 are the amplitudes either side of the spacer layer, t_h and M_h are the respective thickness and saturation magnetization of the hard layer, t_s is the thickness of the spacer and λ is the wavelength of the roughness (which for conformal roughness is considered to be equal to the average in-plane grain size of the hard layer).

From equation (1), using the structural parameters obtained from the x-ray reflectivity and TEM measurements given in table 1, the ferromagnetic coupling field on the (upper) Fe* layer was estimated. The measured coupling field experienced by this layer is given by the displacement of the origin of the minor loop. The measured and estimated values are in good agreement (table 1), suggesting that Néel coupling is the dominant mechanism in these trilayers.

In addition to the shifted minor loops in figure 3, it appears that the reversal of the hard Fe layer has become nonuniform in the trilayer (compare, for example, figures 3(c) and 1(a)). This has been observed in other spin-valve systems [3, 4] and is important because the magnetization reversal will determine the field response of the TMR or GMR in these films. Kerr microscopy measurements performed elsewhere [19] have indicated that this nonuniform reversal can be the result of local regions in the film reversing separately. As a possible explanation for this, we consider here the effect of local variations in the ferromagnetic interlayer coupling on trilayer M–H loops, calculated using a simple phenomenological model. Such variations could occur due to the inhomogeneous nature of the trilayers.

In the model the trilayer is divided into 1000 coupled element pairs and a Gaussian distribution applied to the interlayer coupling *energy* between them. Assuming that the field is applied along an easy axis, and that all elements in the soft and hard layers have the same intrinsic coercivities, H_1^C and H_2^C, respectively, then a given element, i, in the soft layer (layer 1) will reverse when the applied field energy exceeds the sum of the intrinsic switching

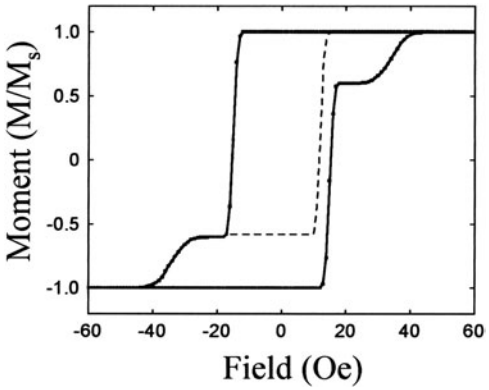

Figure 6. The calculated M–H loop obtained for a model trilayer exhibiting local variations in ferromagnetic interlayer coupling. Model parameters are given in the text.

energy and interlayer coupling energy, i.e.

$$-(\boldsymbol{H}_0 \cdot \boldsymbol{M}_{i,1})t_1 \geqslant H_1^C M_1 t_1 + H_{i,1}^{coup} t_1 \left(\frac{\boldsymbol{M}_{i,1} \cdot \boldsymbol{M}_{i,2}}{M_2} \right) \tag{2}$$

where $\boldsymbol{H}_0$ is the applied field vector, $\boldsymbol{M}_{i,1}$ and $\boldsymbol{M}_{i,2}$ are the local magnetization vectors in the respective soft and hard elements, t_1 is the thickness of the soft layer and M_1 (M_2) is the saturation magnetization of the soft (hard) layer. $H_{i,1}^{coup}$ is the fictitious interlayer coupling *field* on the soft layer element, given by the familiar relation

$$|E_i^C| = H_{i,1}^{coup} M_1 t_1 \tag{3}$$

where E_i^c is the interlayer coupling energy associated with the element pair. If it is assumed that with the field applied along an easy axis, $\boldsymbol{M}_{i,1}$ and $\boldsymbol{M}_{i,2}$ always lie either parallel or antiparallel to $\boldsymbol{H}_0$, then the effective switching field of the soft element is simply $H_1^C \pm H_{i,1}^{coup}$, where the sign depends on the local orientation of $\boldsymbol{M}_{i,1}$ and $\boldsymbol{M}_{i,2}$. Similar expressions are obtained for the reversal of the hard layer elements. By summing the contributions to the total magnetization as a function of applied field, M–H loops can be calculated.

This model has been applied in order to investigate the nonuniform reversal in the trilayers measured here and a qualitative fit to the M–H loop for the trilayer in figure 3(c) is shown in figure 6. In this case, H_1^C was taken from the minor loop in figure 3(c) and is the intrinsic coercivity of the soft layer in the trilayer film (i.e. 13.5 Oe), whereas H_2^C was taken as the coercivity of the single hard Fe layer in figure 1(a) (i.e. 42 Oe). Values of M_1 and M_2 are taken as being equal to that of bulk Fe (VSM measurements revealed saturation magnetization values close to the bulk value for both Fe and Fe* layers). The mean interlayer coupling energy is determined to be 0.015 erg cm^{-2} from the offset of the minor loop in figure 3(c), whilst the standard deviation of the Gaussian was varied until a reasonable qualitative fit was obtained, giving a value of ± 0.01 erg cm^{-2}. It is interesting to note that the model reproduces well the greater nonuniformity of reversal in the thinner layer (in this case the hard Fe layer), due to the surface energy density nature of the interlayer coupling energy (equation (3)). This would tend to support the explanation of the nonuniform reversal being caused by local variations in the interlayer coupling energy.

Given that Néel coupling has been found to be the dominant mechanism in these films, the cause of the local variations in the interlayer coupling is likely to be structural inhomogeneity, i.e. variations in one or more of the parameters given in equation (1). For example, a range of grain sizes between 100 and 350 Å (this determines λ in equation (1)) would lead to the observed value of the standard deviation in the coupling energy distribution. From the micrograph shown in figure 2(b), such a variation in grain sizes would seem plausible.

4. Conclusions

The use of N-doping to reduce the coercivity in the 'free' Fe layer in Fe/AlN/Fe trilayers has been examined. It is found that the presence of a low background partial pressure of N_2 (5×10^{-5} mbar) in the growth chamber is sufficient to magnetically soften the Fe layer by reducing the grain size. Hard/soft spin-valve trilayers were obtained using N-doped and undoped Fe layers. Detailed magnetic and structural characterization reveal the presence of ferromagnetic interlayer coupling that could be well described by a Néel coupling mechanism. It is found that the nonuniform reversal, seen in the M–H loops, can be reproduced in simulated M–H loops by using a simple model in which local regions reverse separately in the applied field owing to variations in the interlayer coupling energy. Such variations are likely to be caused by structural inhomogeneity in the films, such as variations in grain size or spacer thickness.

The use of N-doping to refine the grain structure in the 'free' magnetic layer of spin-valves containing Fe has been demonstrated here. The technique could prove important for tailoring the coercivity of the 'free' layer in spin-valves comprising other high-polarization magnetic layers.

Acknowledgments

The authors would like to thank Mr B Ashworth for TEM specimen preparation, and Dr C A Faunce for TEM cross-sectional analysis. We are also grateful to J D R Buchanan at the University of Durham, for help with the x-ray reflectivity fitting.

References

[1] Chopra H D, Yang D X, Chen P J, Parks D C and Egelhoff W F Jr 2000 *Phys. Rev.* B **61** 9642
[2] Tiusan C, Dimopoulos T, Ounadjela K, Hehn M, van den Berg H A M, da Costa V and Henry Y 2000 *Phys. Rev.* B **61** 580
[3] Tegen S, Mönch I, Schumann J, Vinzelberg H and Schneider C M 2001 *J. Appl. Phys.* **89** 8169
[4] Platt C L, McCartney M R, Parker F T and Berkowitz A E 2000 *Phys. Rev.* B **61** 9633
[5] Hehn M, Lenoble O, Lacour D and Schuhl A 2000 *Phys. Rev.* B **62** 11344
[6] Meservey R and Tedrow P M 1994 *Phys. Rep.* **238** 173
[7] Féry Ch, Hennet L, Lenoble O, Piecuch M, Snoeck E and Bobo J-F 1998 *J. Phys.: Condens. Matter* **10** 6629
[8] Sharma M, Nickel J H, Anthony T C and Wang S X 2000 *Appl. Phys. Lett.* **77** 2219
[9] Bruyère J C, Massanet O, Montmory R and Néel L 1965 *IEEE Trans. Magn.* **1** 10
[10] Kools J C S, Kula W, Mauri D and Lin T 1999 *J. Appl. Phys.* **85** 4466
[11] Néel L 1962 *C. R. Acad. Sci., Paris* **255** 1676
[12] Coey J M D and Smith P A I 1999 *J. Magn. Magn. Mater.* **200** 405
[13] Telling N D, Bonder M J, Jones G A, Faunce C A, Grundy P J, Lord D G and Joyce D E 2001 *IEEE Trans. Magn.* **37** 2308
[14] Herzer G 1991 *Mater. Sci. Eng.* A **133** 1
[15] de Vries G 1959 *Physica* **25** 1211
[16] Liu Y-K, Harris V G and Kryder M H 2001 *IEEE Trans. Magn.* **37** 1779
[17] Fuller H W and Sullivan D L 1962 *J. Appl. Phys.* **33** 1063
[18] Wormington M 1999 *Phil. Trans. R. Soc.* A **357** 2827
[19] Lenoble O, Hehn M, Lacour D, Schuhl A, Hrabovsky D, Bobo J-F, Diouf B and Fert A R 2001 *Phys. Rev.* B **63** 52409